Journal of Computer Science and Artificial Intelligence
ISSN: 3078-8242 (Print), ISSN: 3078-2309 (Online) | Vol. 3, No. 3, 2025

Improved Artificial Potential Field and Model Predictive Control for Autonomous Vehicle Local Path Planning

Wenjie Wu *

College of Electrical and Information Engineering, Lanzhou University of Technology, Lanzhou, 730050, China
* **Corresponding author**: Wenjie Wu (Email: wwj_5114@163.com)

Abstract: In this paper, a local path planning algorithm based on improved artificial potential field (APF) method and model predictive control (MPC) is proposed for the safe driving of autonomous vehicles under complex working conditions. An adjustment factor is introduced to establish a novel obstacle repulsive potential field and an enhanced gravitational potential field, which are then integrated with the MPC algorithm. Secondly, introduce the potential field at the road boundary to ensure that vehicles travel within the safe area of the road. Finally, simulation results demonstrate the effectiveness of the proposed control strategy in ensuring the safe navigation of unmanned vehicles in complex operational environments. Compared with the traditional MPC path planning strategy, this strategy can combine the actual road condition information to establish a more accurate road environment model and finally plan a safe local expected trajectory.

Keywords: Autonomous vehicle; Path planning; Model predictive control; Artificial potential field method.

1. Introduction

In recent years, the advancements in computer and sensor technologies have significantly propelled the progress of autonomous vehicles. Autonomous vehicles play a key role in optimizing resource consumption, energy conservation and emission reduction and improving driving safety. Path planning technology is a fundamental prerequisite for achieving these objectives, where obstacle avoidance capability and path optimality are two core components of the planning algorithm.

Path planning in the field of academic research is usually divided into global and local path planning (Xu et al, 2024; Tu et al, 2024; Zhou et al, 2024; Yao et al, 2024). However, global path planning methods typically use models that ignore the vehicle volume, wheelbase, and dynamic characteristics. As a result, the generated reference paths are difficult to directly apply to the path tracking module of vehicle control systems. As the execution layer of the motion planning system, local trajectory planning utilizes existing local path planning algorithms to generate trajectories in real time that adhere to vehicle dynamic constraints. Therefore, local path planning is an important link to ensure the driving safety of autonomous vehicles. At present, local path planning algorithms are primarily classified into four categories: the curve fitting method (Igneczi et al, 2024), the spatial sampling method (Lim et al, 2018), the graph search method (De Filippis and Guglieri, 2012), and the numerical optimization method (Roald, 2015).

Spatial sampling is a key technique for obstacle avoidance in autonomous driving, enabling effective handling of complex and dynamic environments. Through dense sampling of the drivable area and path evaluation, this method allows autonomous vehicles to generate feasible trajectories for navigating diverse and challenging road conditions. The graph search method is a computational technique employed in autonomous systems to generate collision-free trajectories through structured environmental representations. The numerical optimization method formulates local path planning as a mathematical program to generate dynamically feasible trajectories for autonomous vehicles under environmental constraints. Sun and Zhu (2025) proposed a novel path planning method by integrating the APF and MPC algorithms. Through global optimization and prediction of future states, this approach ensures smooth vehicle motion while preventing issues such as entrapment in local minima and unreachable goals. Compared to the conventional APF, safe artificial potential field (SAPF) can reach the target location in a shorter time, providing a shorter and smoother path with a minimum distance to the obstacle less than the assumed value Szczepanski. (2023). Guan et al. (2025) proposed a bidirectional APF-RRT* algorithm to address limitations in the traditional RRT* method, such as high sampling randomness, slow convergence speed, and insufficient path smoothness. By incorporating a improved APF approach, this method enhances the exploration capability of the random tree, enabling it to rapidly escape local optima and consequently improve path quality.

The MPC algorithm possesses the capability to function as a path planning algorithm as well. She et al. (2025) proposed a path planning algorithm for multi-wheeled mobile robots in uncertain environments, integrating the APF method with MPC to ensure safe and smooth driving. This paper utilizes a genetic algorithm to optimize the controller parameters. Nguyen et al. (2023) proposed an autonomous emergency steering control strategy utilizing linear time-varying model predictive control (LTV-MPC) to predict state behavior near operating points over the prediction horizon. This method effectively adapts to changes in the system model while satisfying state and control constraints.

While most research endeavors on autonomous vehicles have concentrated on path tracking control, they have largely overlooked the challenge of active obstacle avoidance in complex operational scenarios. Building upon the aforementioned references, this paper establishes a path planning algorithm based on the improved APF method and

MPC to realize the local path planning of autonomous vehicles.

The key highlights of this research are summarized below:

According to the real-time road information, the improved APF method is combined with the MPC algorithm. This work overcomes inherent limitations in conventional approaches, such as local optima and unreachable targets.

A novel MPC-based path planner is proposed, embedding environmental potential fields in the optimization objective. The algorithm outputs real-time trajectories that satisfy vehicle dynamics constraints and guarantee collision avoidance under actual road scenarios.

2. Environmental Potential Field Modeling

Conventional APF methods exhibit two fundamental limitations in path planning: target inaccessibility and local minima. Target inaccessibility occurs when residual repulsive forces from nearby obstacles prevent vehicle stabilization at the goal position, while local minima arise from either excessive angular deviation between attraction/repulsion vectors or force equilibrium in multi-obstacle environments where cumulative repulsion collinearly opposes goal attraction. The above analysis indicates that the traditional APF method has obvious theoretical limitations in the application of path planning and is not suitable for direct citation in this paper. Therefore, this paper proposes an improved APF method to resolve these limitations in conventional approaches.

2.1. Improve the Repulsive Potential Field

The traditional repulsive potential field function can be expressed as:

$$U_{req}(x,y)=\begin{cases}\frac{1}{2}K_{req}\left(\frac{1}{\sqrt{|x-x_t|^2+|y-y_t|^2}}-\frac{1}{d_0}\right)^2 & 0\le\sqrt{|x-x_t|^2+|y-y_t|^2}\le d_0\\ 0 & \sqrt{|x-x_t|^2+|y-y_t|^2}\ge d_0\end{cases} \tag{1}$$

Where, K_{req} is the repulsive potential gain coefficient, and d_0 is the influence range of the obstacle.

The corresponding repulsive force $F_{req}(x,y)$ is the negative gradient of the repulsive field.

When $0\le\sqrt{|x-x_t|^2+|y-y_t|^2}\le d_0$

$$F_{req}(x,y)=K_{req}\left(\frac{1}{\sqrt{|x-x_t|^2+|y-y_t|^2}}-\frac{1}{d_0}\right)\frac{1}{\left[(x-x_t)^2+(y-y_t)^2\right]}\times\nabla\sqrt{|x-x_t|^2+|y-y_t|^2} \tag{2}$$

When $\sqrt{|x-x_t|^2+|y-y_t|^2}\ge d_0$

$$F_{req}(x,y)=0 \tag{3}$$

To solve the limitations of conventional APF methods, this paper introduces adjustment factor η^n into the repulsive force potential field function This modification ensures simultaneous convergence of repulsive and attractive forces to zero at the target point, effectively resolving goal non-reachability and local minima issues.

Improved repulsive force field function:

$$\bar{U}_{req}(x,y)=\begin{cases}\frac{1}{2}\bar{K}_{req}\left(\frac{1}{\sqrt{|x-x_t|^2+|y-y_t|^2}}-\frac{1}{\rho_0}\right)^2\eta^n & 0\le\sqrt{|x-x_t|^2+|y-y_t|^2}\le d_0\\ 0 & \sqrt{|x-x_t|^2+|y-y_t|^2}\ge d_0\end{cases} \tag{4}$$

where, η^n is the power of the distance between the vehicle and the target point, and n is a positive integer.

The corresponding repulsive force is:

$$F_{reo1}=\bar{K}_{req}\left(\frac{1}{\sqrt{|x-x_t|^2+|y-y_t|^2}}-\frac{1}{d_0}\right)\frac{\eta^n}{(x-x_t)^2+(y-y_t)^2} \tag{5}$$

The adjustment factor η^n enables dynamic modulation of the repulsive field. Additionally, this paper introduces a paradoxical repulsive force F_{reo2} generated by obstacles yet oriented toward the goal point. This design effectively mitigating local minima problems. The expression of F_{reo2} is shown as Eq (6). Fig. 1 shows the force distribution of the vehicle in the improved potential field environment.

$$F_{reo2}=\frac{n}{2}K_{req}\left(\frac{1}{\sqrt{|x-x_t|^2+|y-y_t|^2}}-\frac{1}{d_0}\right)^2\eta^{n-1} \tag{6}$$

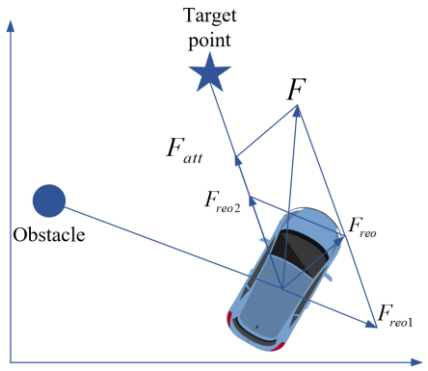

Figure 1. Force Analysis Schematic of an Autonomous Vehicle under Improve APF

When the vehicle fails to reach the target point, the corresponding repulsive force is expressed as follows:

$$F_{reo}(x,y)=\begin{cases}(F_{reo1}+F_{reo2})\nabla\sqrt{|x-x_t|^2+|y-y_t|^2} & 0\le\sqrt{|x-x_t|^2+|y-y_t|^2}\le d_0\\ 0 & \sqrt{|x-x_t|^2+|y-y_t|^2}\ge d_0\end{cases} \tag{7}$$

Where, the direction of F_{reo1} is pointing from the obstacle to the vehicle, and the direction of F_{reo2} is pointing from the vehicle to the target point.

Fig. 2 illustrates the 3D repulsive potential field distribution derived from Eq. (4) for a 150 m × 7 m urban two-lane road section.

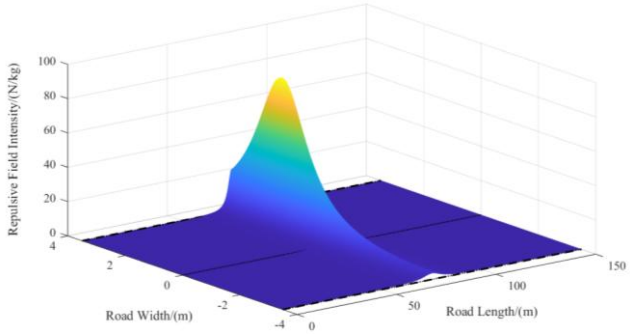

Figure 2. 3D repulsive potential field distribution

2.2. Improve the Gravitational Potential Field

While conventional gravitational potential fields in APF methods depend solely on the distance between autonomous vehicles and the goal point, practical navigation requires post-obstacle avoidance recovery to the original lane. To address this limitation, this paper set the vehicle's current position as the trajectory origin, define the terminal point at lateral offset y_d, and establish monotonically decreasing potentials along the lane orientation. The improved gravitational potential field is formulated as:

$$\bar{U}_{att}=\bar{K}_{att}\sqrt{|x-x_0|^2+|y-y_{\max}|^2} \tag{8}$$

Where, $\bar{K}_{att}$ represents the improved gravitational potential energy gain coefficient, x_0 represents the lateral coordinate position of the vehicle at the starting point, and $y_{\max}$ represents the maximum lateral distance of the driving area.

Fig. 3 illustrates the 3D gravitational potential field distribution derived from Eq. (8) for a 150 m × 7 m urban two-lane road section.

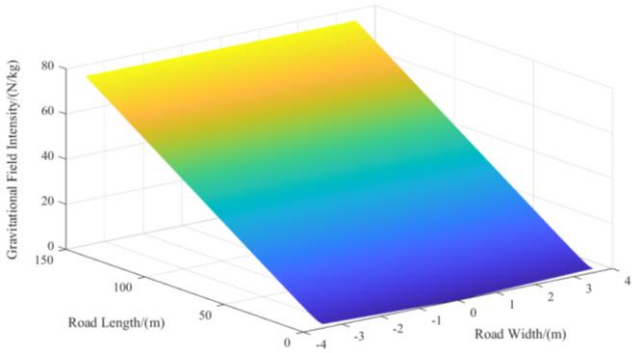

Figure 3. 3D gravitational potential field distribution

2.3. Road Boundary Potential Field

For structured road scenarios, this paper introduces a road-boundary repulsive field. This field dynamically adjusts repulsive magnitude based on the Euclidean distance between autonomous vehicles and road boundaries, ensuring persistent confinement within central safe zones.

Given lane width d and vehicle width w. Fig. 4 is a schematic diagram of the potential field at the vehicle road boundary

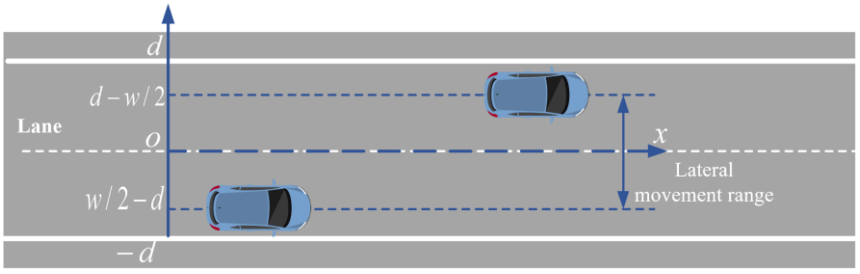

Figure 4. Schematic diagram of the potential field at the vehicle road boundary

The repulsive potential field at the road boundary is expressed as follows:

$$U_{req,edge}=\begin{cases}K_{edge}\left(y-d\right)^{-2}, & d-\dfrac{w}{2}<y\le d\\ K_{line}ve^{-y^2}, & \dfrac{w}{2}-d<y\le d-\dfrac{w}{2}\\ K_{edge}\left(y-d\right)^{-2}, & -d<y\le\dfrac{w}{2}-d\end{cases}\tag{9}$$

Where, K_{edge} is the potential energy gain coefficient of the road boundary, K_{line} is the potential energy gain coefficient of the center lane line, v is the vehicle speed, and y is the lateral coordinate of the vehicle.

Fig. 5 illustrates the 3D road boundary potential field distribution derived from Eq. (9) for a 150 m × 7 m urban two-lane road section.

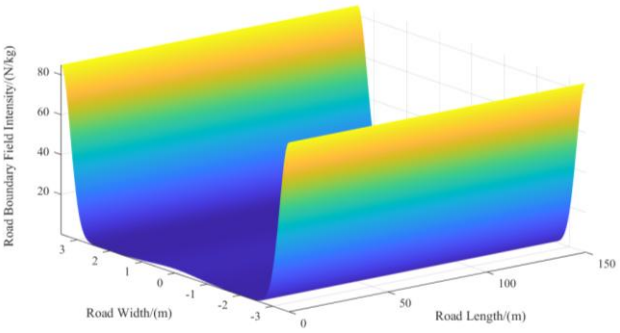

Figure 5. 3D road boundary potential field distribution

2.4. Environmental Potential Field Modeling

Aiming at the problems such as local minima and unreachable targets existing in the traditional APF method, this paper constructs a new potential field function, and the function expression is as follows:

$$U=\bar{U}_{att}+\bar{U}_{req}+U_{req,edge}\tag{10}$$

3. Design of Model Predictive Controller

3.1. Point Mass Model

The selection of vehicle models requires comprehensive consideration of factors such as performance and computational load. Therefore, considering the vehicle model in the local path planner comprehensively, the computational performance should be taken into account while meeting the real-time and robustness. Ultimately, the point mass model with less computational complexity was selected (Li and Feng, 2020). The analysis of the vehicle's force conditions ignoring the vehicle body size information is shown in Fig. 6:

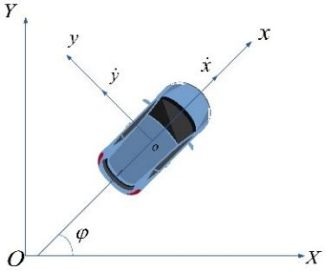

Figure 6. Point Mass Model

Where (x,y) and (X,Y) are expressed as the coordinate systems for the body and the ground, respectively, and φ is the vehicle yaw angle.

The vehicle point mass is modelled in the geodetic reference coordinate system.

$$\begin{cases}\dot{\dot{x}}=a_x,\ \dot{\dot{y}}=a_y\\ \varphi=\dfrac{a_y}{\dot{x}}\\ \dot{Y}=\dot{x}\sin\varphi+\dot{y}\cos\varphi\\ \dot{X}=\dot{x}\cos\varphi-\dot{y}\sin\varphi\end{cases}\tag{11}$$

3.2. Safety Collision Distance Model Establishment

The planner state variable is defined as $\xi=\left[\dot{x},\dot{y},\varphi,Y,X\right]^T$, select $u=a_y$ as the control quantity.

Using the system state transition function, the system described by Eq. (1) is further simplified as follows:

$$\dot{\xi}(t)=f\left(\xi(t),u(t)\right)\tag{12}$$

Where $f(\cdot)$ denotes the state transfer function of the system.

Utilizing the forward Euler method, we convert the point mass model into a nonlinear discrete prediction model.

$$\xi(k+1)=\xi(k)+Tf\left(\xi(k),u(k)\right)\tag{13}$$

Where T denotes the sampling period of local path planning.

We define the prediction output vector for the future N_p step, along with the prediction input vector for the N_c step.

$$Y=\begin{bmatrix}\eta(k+1|t_0)\\ \eta(k+2|t_0)\\ \text{L}\\ \eta(k+N_c|t_0)\\ \text{L}\\ \eta(k+N_p|t_0)\end{bmatrix},\quad U=\begin{bmatrix}u(k|t_0)\\ u(k+1|t_0)\\ \text{L}\\ u(k+N_c-1|t_0)\end{bmatrix}$$

Then, the output of the prediction in the future N_p step for the local path planning system can be derived using the following formulation.

$$Y=F\left(\xi(k|t_0),U\right)\tag{14}$$

In order to avoid vehicle sliding, $|a_y|<ug$ is added as a vehicle dynamic constraint.

3.3. Optimization Problem Construction and Solution

For the path planner, the environment model established by the improved APF method is introduced into the MPC objective function. The specific form of the new objective function of the path planner is as follows:

$$J=\sum_{i=1}^{N_P}\left\|\eta\left(k+i|k\right)-Y_{ref}\left(k+i|k\right)\right\|_Q^2+\sum_{j=1}^{N_C}\left\|u\left(k+i|k\right)\right\|_R^2+\sum_{i=1}^{N_P}\left\|U\left(k+i|k\right)\right\| \tag{15}$$

Where $U(k+i)$ represents the predicted potential energy value of the road environment at k for the future $k+i$.

The newly established objective function mainly consists of the following three parts:

The first part is the deviation of the predicted output vector from the reference trajectory.

The second part is the size of the control input.

The third part is the road environment potential field.

3.4. Quintuple Polynomial Curve Fitting

In the trajectory replanning algorithm, the objective function minimizes the cumulative distance deviation between reference points over a finite horizon. The algorithm outputs a sequence of discrete trajectory points within the predicted horizon. These replanned waypoints are fitted using a quintic polynomial expressed as:

$$\begin{cases} Y=a_0t^5+a_1t^4+a_2t^3+a_3t^2+a_4t+a_5 \\ \varphi=b_0t^5+b_1t^4+b_2t^3+b_3t^2+b_4t+b_5 \end{cases} \tag{16}$$

Where $a_i, b_i\,(i=1,2,3,4,5)$ are the parameters of the desired trajectory fit and heading angle fit.

4. Simulation Analysis

To validate the efficacy of the proposed improved APF method integrated with MPC, simulation studies were conducted using the MATLAB/Simulink platform. A simulated environment spanning 150 m × 7 m was constructed, corresponding to standard dimensions of a single-direction urban road with dual lanes. Parameters of the road environment model and vehicle dynamics model are summarized in Table 1.

Table 1. Parameters of the road environment model and vehicle dynamics model

Vehicle Parameters	Parameter Values	Parameter Definitions
M	$1416kg$	Total vehicle mass
$\bar{K}_{rep}$	100	Repulsive potential gain coefficient
$\bar{K}_{att}$	0.5	Improved gravitational potential gain coefficient
K_{redge}	2	Road boundary potential gain coefficient
K_{line}	10	Road centerline attractive gain coefficient
d	$3.5m$	Single-Lane width
L	$150m$	Road length

Secondly, obstacle vehicles and target points were configured: three rectangular obstacles approximating standard passenger vehicle dimensions (5m×1.6m) were positioned at coordinates $(30,1.8)$, $(50,-1.8)$, and $(130,1.8)$. The target point was located at position $(120,1.8)$. To validate whether the improved APF method resolves limitations of conventional APF, an additional obstacle vehicle was placed near the target point at coordinate $(130,1.8)$. Finally, the controlled vehicle's initial position was set at $(0,1.8)$, with the proposed control strategy generating a collision-free reference trajectory.

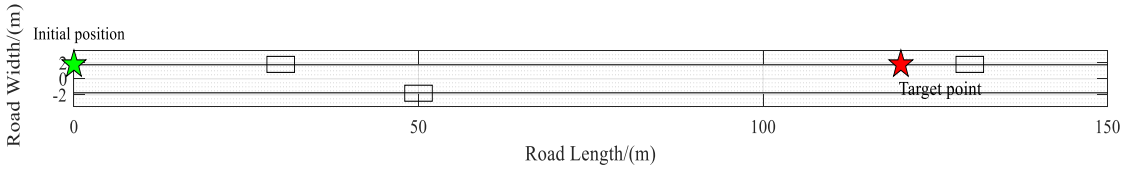

Figure 7. Map environment schematic diagram

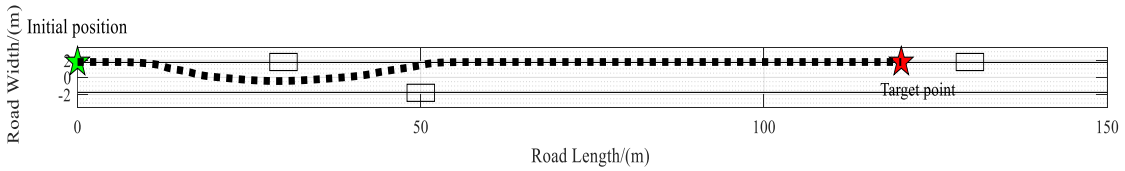

Figure 8. Schematic diagram of Path planning

Fig. 7 illustrates the constructed urban single-direction dual-lane road environment. Fig. 8 displays a collision-free reference trajectory (denoted by a black dash-dotted line) generated under the proposed control strategy. As evidenced in Fig. 8, the controlled vehicle successfully navigated from its initial position to the target while circumventing obstacles near the destination without trajectory distortion. This outcome confirms that the improved APF method effectively resolves the limitations inherent in conventional APF approaches, thereby validating the efficacy of the local path planning algorithm.

5. Conclusions

Firstly, the traditional APF method was improved, and then the improved APF method was combined with the MPC algorithm to solve the limitations of the traditional APF method such as local optimum and target unreachable. Secondly, the environmental model established by the improved APF method is introduced into the predictive control objective function of the model. This environmental model takes into account the potential field at the road

boundary and ensures that vehicles can travel within the safe area in the center of the road. Meanwhile, different road potential field models can be established according to the driving environment of the vehicle to ensure that the vehicle safely avoids obstacles while complying with traffic driving regulations. Finally, based on the simulation analysis, the improved APF method solves the problems existing in the traditional APF method. It can be combined with the actual road condition information to establish a more accurate road environment model and ultimately plan a safe local expected trajectory.

References

[1] De Filippis L, Guglieri G. (2012) Advanced graph search algorithms for path planning of flight vehicles. Recent Advances in Aircraft Technology: 159-192.

[2] Guan T, Han Y, Kong M et al. (2025) An improved artificial potential field with RRT star algorithm for autonomous vehicle path planning. Scientific Reports 15(1): 1-21.

[3] Igneczi G F, Horvath E, Toth R et al. (2024) Curve trajectory model for human preferred path planning of automated vehicles. Automotive Innovation 7(1): 59-70.

[4] Li S and Feng X (2020). Study of structural optimization design on a certain vehicle body-in-white based on static performance and modal analysis. Mechanical Systems and Signal Processing 135: 106405.

[5] Lim W, Lee S, Sunwoo M et al. (2018) Hierarchical trajectory planning of an autonomous car based on the integration of a sampling and an optimization method. IEEE Transactions on Intelligent Transportation Systems 19(2): 613-626.

[6] Nguyen H D, Kim D, Son Y S et al. (2023) Linear time-varying mpc-based autonomous emergency steering control for collision avoidance. IEEE Transactions on Vehicular Technology 72(10): 12713-12727.

[7] Roald A L. (2015) Path planning for vehicle motion control using numerical optimization methods. NTNU.

[8] She Y, Song C, Sun Z et al. (2025) Optimized Model Predictive Control-Based Path Planning for Multiple Wheeled Mobile Robots in Uncertain Environments. Drones 9(1): 39.

[9] Sun Q, Zhu K. (2025) Path planning and tracking system based on MPC-APF-EKF for autonomous vehicle local obstacle avoidance. Engineering Research Express 7(2): 025211.

[10] Szczepanski R (2023) Safe artificial potential field - novel local path planning algorithm maintaining safe distance from obstacles. IEEE Robotics and Automation Letters 8(8): 4823-4830.

[11] Tu H, Deng Y, Li Q et al (2024). Improved RRT global path planning algorithm based on Bridge Test. Robotics and Autonomous Systems 171: 104570.

[12] Xu X, Zeng J, Zhao Y et al. (2024) Research on global path planning algorithm for mobile robots based on improved A. Expert Systems with Applications 243: 122922.

[13] Yao M, Deng H, Feng X et al. (2024) Improved dynamic windows approach based on energy consumption management and fuzzy logic control for local path planning of mobile robots. Computers & Industrial Engineering 187: 109767.

[14] Zhou Q, Lian Y, Wu J et al. (2024) An optimized Q-Learning algorithm for mobile robot local path planning. Knowledge-Based Systems 286: 111400.